ELSEVIER

Applied Ocean Research 23 (2001) 93–101

Applied Ocean Research

www.elsevier.com/locate/apor

Dynamic tension of cables in a random sea: analytic approximation for the envelope probability density function

J.A.P. Aranha[a,*], M.O. Pinto[b], A.J.P. Leite[b]

[a]*Department of Naval Engineering, USP, CP61548, Sao Paulo, Brazil*
[b]*E and P, Petrobras, Rio de Janeiro, Brazil*

Received 20 June 2000; revised 20 March 2001

Abstract

When a random sea is filtered by the transfer function of a floating system a narrow banded excitation at the suspended end of risers and mooring lines is, in general, obtained. Using then this gaussian narrow banded signal as input and the algebraic expression for the dynamic tension derived in Aranha and Pinto [Dynamic tension in risers and mooring lines: an algebraic approximation for harmonic excitation (2001), submitted], the probability density function (pdf) for the envelope of the dynamic tension in the risers and mooring lines can be analytically approximated. The obtained expression differs, in general, from the Rayleigh distribution and it is compared, in the present work, with numerical results in the time domain, the agreement being fair even in the cases where the risers become dynamically compressed. From a more practical point of view, given then the transfer function of the floating body and the wave energy spectrum, the statistics of the dynamic tension can be estimated directly from some few integral parameters of the static configuration introduced in Aranha and Pinto [Dynamic tension in risers and mooring lines: an algebraic approximation for harmonic excitation (2001), submitted], avoiding the simulation in time of the riser's dynamics.

Keywords: Probability density function; Dynamic tension; Cable

1. Introduction

Risers and mooring lines, anchored in a floating system, are dynamically excited by *random sea waves*, in general modeled as being a *gaussian process*, see Refs. [1,2]. However, the relation between the basic input, the sea wave, and the dynamic tension in the cable is non-linear, mainly due to the viscous dissipation caused by the cable motion in water. The non-linearity distorts the gaussian property of the input and, as a consequence, the envelope of the dynamic tension does not follow, in general, the usual Rayleigh distribution of the linear systems excited by a gaussian process. One should resort to long time domain simulations to obtain statistical information about the dynamic tension, an effort that besides to be tedious is not free of uncertainties, mainly because sometimes the numerical codes present difficulties when simulating a high sea state, as discussed in Ref. [3].

On the other hand, the sea wave is filtered by the floating body transfer function, resulting in a random displacement $U(t)$ in the direction of the cable's tangent at the suspended end that, besides to be gaussian, is narrow banded. It turns out then that $U(t)$ is a quasi-harmonic random excitation and, in this context, the envelope of the dynamic tension can be estimated by the algebraic approximation derived in Ref. [3]. Once a relation between the envelopes of the dynamic tension and of the displacement $U(t)$ is established, it is a trivial exercise to obtain the probability density function (pdf) for the envelope of the dynamic tension, since the envelope of $U(t)$ follows the standard Rayleigh distribution.

This is the objective of the present work. In Section 2, some basic results about the envelope of a narrow banded random signal are recovered and the probability density function for the envelope of the dynamic tension is derived; in Section 3, the obtained expression is checked against numerically determined probability density functions using the ORCAFLEX program and in Section 4 the conclusions are presented.

2. Probability density function for the envelope of the tension

Suppose a harmonic wave with unit amplitude, frequency ω and incident in a direction β, and let $H_U(\omega,\beta)$ be the

* Corresponding author. Address: Department of Naval and Ocean Engineering, Cidade University, EPSUP, CEP 05508-900, Sao Paulo, Brazil. Tel.: +55-11-3818-5340; fax: +55-11-3818-5717.
E-mail address: japaran@usp.br (J.A.P. Aranha).

0141-1187/01/$ - see front matter
PII: S0141-1187(01)00010-4

floating body transfer function, relating this wave to the tangent displacement $U(t)$ at the cable suspended end. A random gaussian sea wave, incident in the direction β and with an energy spectrum $S(\omega)$, causes a random gaussian displacement $U(t)$ with spectrum $S_U(\omega)$ given by

$$S_U(\omega) = |H_U(\omega,\beta)|^2 S(\omega). \tag{2.1a}$$

Introducing the spectral moments

$$m_{j,U} = \int_0^\infty \omega^j S_U(\omega)\,\mathrm{d}\omega, \qquad j = 0,1,2,\ldots. \tag{2.1b}$$

the *standard deviation* σ_U, the *central frequency* ω_U and the *averaged frequency* $\omega_{Z,U}$ are defined by the expressions:

$$\sigma_U = m_{0,U}^{1/2}, \qquad \omega_U = \frac{m_{1,U}}{m_{0,U}}, \qquad \omega_{Z,U} = \sqrt{\frac{m_{2,U}}{m_{0,U}}}. \tag{2.1c}$$

Following Ref. [2], the bandwidth of the random signal $U(t)$ can be gauged by the non-dimensional parameter

$$\nu_U = \sqrt{\left(\frac{\omega_{Z,U}}{\omega_U}\right)^2 - 1}, \tag{2.2}$$

where obviously, $\nu_U = 0$ for a harmonic signal, since $\omega_{Z,U} = \omega_U$. The basic assumption in the present work is that the floating system transfer function filters the wave input, rendering the imposed displacement $U(t)$ *narrow banded* ($\nu_U \ll 1$); this assumption will be verified in the present work, where the transfer function of an actual system will be used in the examples.

A realization of the random signal $U(t)$ with duration T_R can be expressed in the form of the Fourier series

$$U(t) = \sum U_n \cos(\omega_n t + \varphi_n), \qquad \omega_n = n\Delta\omega, \qquad \Delta\omega = 2\pi/T_R. \tag{2.3a}$$

The random phases $\{\varphi_n;\ n = 1,2,\ldots\}$ being uniformly distributed in the interval $(0,2\pi)$ and the random amplitudes $\{U_n;\ n = 1,2,\ldots\}$ obeying the Rayleigh distribution with $E[U_n^2] = 2S_U(\omega_n)\Delta\omega$. Let now $V(t)$ be the Hilbert transform of $U(t)$, given by

$$V(t) = \frac{1}{\pi} PV \int_{-\infty}^{\infty} \frac{U(s)}{t-s}\,\mathrm{d}s = \sum U_n \sin(\omega_n t + \varphi_n) \tag{2.3b}$$

and $U_0(t)$ be defined as

$$U_0(t) = \sqrt{U^2(t) + V^2(t)}. \tag{2.3c}$$

Introducing the functions

$$U_S(t) = \sum U_n \cos(\Omega_n t + \varphi_n), \qquad V_S(t) = \sum U_n \sin(\Omega_n t + \varphi_n), \qquad \Omega_n = \omega_n - \omega_U \tag{2.4a}$$

one can easily check that

$$U(t) = \cos(\omega_U t)U_S(t) - \sin(\omega_U t)V_S(t), \qquad V(t) = \cos(\omega_U t)V_S(t) + \sin(\omega_U t)U_S(t) \tag{2.4b}$$

and so

$$U_0(t) = \sqrt{U_S^2(t) + V_S^2(t)}. \tag{2.4c}$$

If now the phase $\varphi(t)$ is defined by the relations

$$\cos\varphi(t) = \frac{U_S(t)}{U_0(t)}, \qquad \sin\varphi(t) = \frac{V_S(t)}{U_0(t)}, \tag{2.4d}$$

then the displacement $U(t)$ can be written in the form

$$U(t) = U_0(t)\cos(\omega_U t + \varphi(t)). \tag{2.5}$$

If $\langle\cdot\rangle$ is the time average operator, it is now an easy task to check that

$$\left\langle\left(\frac{\mathrm{d}U_S(t)}{\mathrm{d}t}\right)^2\right\rangle^{1/2} = \nu_U\omega_U\left\langle U_S^2(t)\right\rangle^{1/2}, \qquad \left\langle\left(\frac{\mathrm{d}V_S(t)}{\mathrm{d}t}\right)^2\right\rangle^{1/2} = \nu_U\omega_U\left\langle V_S^2(t)\right\rangle^{1/2}$$

and so, from Eqs. (2.4c) and (2.4d), it follows that the *envelope*[1] $U_0(t)$ and the *phase* $\varphi(t)$ in Eq. (2.5) change slowly in time for a narrow banded process ($\nu_U \ll 1$). In this case, the displacement $U(t)$ is *quasi-harmonic* and, in this context, the algebraic approximation derived in Ref. [3] can be used to estimate the dynamic tension. This point will be elaborated next.

Consider thus the quasi-harmonic input (2.5) and let $a(t) = U_0(t)/\sigma_U$ be the normalized envelope of $U(t)$; the envelope $T_D(s,t)$ of the dynamic tension can be approximated, in this context, by the harmonic results (2.8a) and (2.8b) obtained in Ref. [3], or

$$\tau(s,t) = \left[\frac{c_1(s)\left(\sqrt{b^2(\Omega) + (4\zeta_0^2/\Omega^4)a^2(t)} - b(\Omega)\right)^2 + 2c_2(s)\left(\sqrt{b^2(\Omega) + (4\zeta_0^2/\Omega^4)a^2(t)} - b(\Omega)\right)}{(4\zeta_0^2/\Omega^4)}\right]^{1/2}, \tag{2.6a}$$

$$\tau(s,t) = \frac{T_D(s,t)}{T_e}, \qquad T_e = EA\frac{\sigma_U}{l+l'},$$

where $(l + l')$ is the cable's *effective length* and $\{\zeta_0;\ \Omega;\ b(\Omega);\ c_{1,2}(s)\}$ are defined in Eqs. (2.5), (2.7c) and (2.8c) of Ref. [3]; however, in these expressions the central frequency ω_U, see Eq. (2.1c), is used in the place of ω in these expressions. The *dynamic tension* $\hat{T}_D(s,t)$ is then

[1] An enlightened discussion about 'wave envelope' is given in Ref. [14].

given by

$$\hat{T}_{\mathrm{D}}(s,t) = T_{\mathrm{D}}(s,t)\cos(\omega_U t + \phi(s,t)) \tag{2.6b}$$

with $T_{\mathrm{D}}(s,t)$ defined in Eq. (2.6a) and $\phi(s,t)$ being the random phase. Observing that both $T_{\mathrm{D}}(s,t)$ and $\phi(s,t)$ vary *slowly in time*, from Eq. (2.6b) it follows that

$$\left(\frac{\mathrm{rms}\hat{T}_{\mathrm{D}}(s,t)}{T_{\mathrm{e}}}\right)^2 = E\left[\frac{\omega_U}{2\pi}\int_t^{t+2\pi/\omega_U} \tau^2(s,t)\cos^2(\omega_U\xi + \phi(s,t))\,d\xi\right] = \frac{1}{2}E[\tau^2(s,t)]$$

and so

$$\mathrm{rms}\hat{T}_{\mathrm{D}}(s,t) = T_{\mathrm{e}}\sigma_\tau(s), \qquad \sigma_\tau^2(s) = \frac{1}{2}E[\tau^2(s,t)]. \tag{2.6c}$$

The variable $a(t)$, being the normalized envelope of the gaussian variable $U(t)$, follows the normalized Rayleigh distribution $p_{\mathrm{R}}(a) = a\exp(-a^2/2)$ and it is now a simple exercise to obtain, from Eqs. (2.6a)–(2.6c), the probability density function $p_\tau(\tau;s)$ of the dynamic tension envelope $\tau(s,t)$. In fact, introducing the functions

$$f(a) = \sqrt{b^2(\Omega) + (4\zeta_0^2/\Omega^4)a^2} - b(\Omega),$$

$$\tau(f) = \frac{\Omega}{2\zeta_0}\left[c_1(s)f^2 + 2c_2(s)f\right]^{1/2}$$

and using the relations

$$p_{\mathrm{f}}(f) = \left(a\frac{\mathrm{d}a}{\mathrm{d}f}\right)\mathrm{e}^{-a^2(f)/2}, \qquad p_\tau(\tau) = p_{\mathrm{f}}(f(\tau))\frac{\mathrm{d}f}{\mathrm{d}\tau}(\tau).$$

It is easy to check that

$$p_\tau(\tau;s) = \frac{1}{c_1(s)}\,\mathrm{e}^{\gamma^2/2}\frac{\tau}{\sqrt{[c_2(s)/c_1(s)]^2 + [b^2(\Omega)/(\gamma^2 c_1(s))]\tau^2}} \times F(\tau)\,\mathrm{e}^{-(\gamma^2F^2(\tau))/2b^2(\Omega)},$$

$$\gamma = \frac{\Omega^2 b(\Omega)}{2\zeta_0},$$

$$F(\tau) = \sqrt{\left(\frac{c_2(s)}{c_1(s)}\right)^2 + \left(\frac{b^2(\Omega)}{\gamma^2 c_1(s)}\right)\tau^2} - \frac{c_2(s)}{c_1(s)} + b(\Omega). \tag{2.7a}$$

From Eq. (2.7a) it follows that the normalized standard deviation $\sigma_\tau(s)$ of the dynamic tension $\hat{T}_D(s,t)$, introduced in Eq. (2.6c), is given by

$$\sigma_\tau(s) = c_1^{1/2}(s)\left\{\left[1 - \gamma^2\left(\frac{1}{b(\Omega)}\frac{c_2(s)}{c_1(s)} - 1\right)\right] + \gamma\left(\frac{1}{b(\Omega)}\frac{c_2(s)}{c_1(s)} - 1\right)G(\gamma^2/2)\right\}^{1/2} \tag{2.7b}$$

the function $G(\cdot)$ being defined by the integral

$$G(x) = \mathrm{e}^x\int_x^\infty \sqrt{2t}\,\mathrm{e}^{-t}\,\mathrm{d}t. \tag{2.7c}$$

With Eqs. (2.7b) and (2.7c) the standard deviation of the dynamic tension can be determined, see Eq. (2.6c), and the *normalized envelope* $r(s,t)$ can be introduced by the expression

$$r(s,t) = \frac{T_{\mathrm{D}}(s,t)}{\mathrm{rms}(\hat{T}_{\mathrm{D}}(s,t)).} \tag{2.8a}$$

The related probability density function being given by

$$p_{\mathrm{E}}(r;s) = \frac{\sigma_\tau^2(s)}{c_1(s)}\,\mathrm{e}^{\gamma^2/2}\frac{r}{\sqrt{[c_2(s)/c_1(s)]^2 + [(b^2(\Omega)\sigma_\tau^2(s))/(\gamma^2 c_1(s))]r^2}} \times F(r)\,\mathrm{e}^{-(\gamma^2F^2(r))/2b^2(\Omega)}, \gamma = \frac{\Omega^2 b(\Omega)}{2\zeta_0},$$

$$F(r) = \sqrt{\left(\frac{c_2(s)}{c_1(s)}\right)^2 + \left(\frac{b^2(\Omega)\sigma_\tau^2(s)}{\gamma^2 c_1(s)}\right)r^2} - \frac{c_2(s)}{c_1(s)} + b(\Omega). \tag{2.8b}$$

As shown by Triantafyllou et al. [4] and discussed in Ref. [3], either in high frequency limit or else when the amplitude of the imposed displacement becomes very large, the cable almost freezes in its equilibrium position, due to the action of the viscous dissipation, and the imposed displacement is absorbed elastically by the cable; since $U(t) = \sigma_U a(t)$ and $\zeta_0 \to \infty$ as σ_U does, then one has (see Eq. (2.9a) in Ref. [3])

$$T_{\mathrm{D}}(s,t) \to T_{\mathrm{e}}a(t), \qquad (\omega_U/\omega_{\mathrm{c}};\sigma_U/D) \gg 1.$$

From this expression it follows that $\{\sigma_\tau(s) \to 1;\ r(s,t) \to a(t)\}$ in these limits and, in particular, one has that $p_{\mathrm{E}}(r) \to p_{\mathrm{R}}(r) = r\exp(r^2/2)$. These results can be recovered from the above expressions, as elaborated next. In fact, when $\Omega \gg 1$ (but keeping $\omega_U/\omega_{\mathrm{e}} \ll 1$) then, with an error of the form $[1 + \mathrm{O}((\omega_U/\omega_{\mathrm{e}})^2;1/\Omega^2)]$, it can be seen that $\{c_1(s) = 1;\ b(\Omega) = c_2(s) = 1 + \zeta_c^2;\ \gamma = O(\Omega^2) \gg 1\}$ and so $G(\gamma^2/2) \cong \gamma$; from Eq. (2.7b) it follows that $\sigma_\tau(s) = 1$ and from Eq. (2.8b) that $p_{\mathrm{E}}(r) = p_{\mathrm{R}}(r) = r\exp(r^2/2)$. If $\sigma_U \to \infty$ $(\zeta_0 \to \infty)$ one has that $\gamma \to 0$ and so, again, $\{\sigma_\tau(s) = 1;\ p_{\mathrm{E}}(r) = p_{\mathrm{R}}(r)\}$.

So far it has been assumed that the dynamic tension is given by the quasi-harmonic expression (2.6b). As the

amplitude and frequency increase, however, the dynamic tension becomes large and the riser can be dynamically compressed; in this case the compressive force *saturates* at the *critical value* $P_{cr}(s)$ defined by (see Ref. [5])

$$P_{cr}(s) = \beta_{cr}(\chi(s))\sqrt{(m + m_a)\mathrm{EJ}}\omega_U, \tag{2.9a}$$

where $\chi(s)$ is the static curvature and β_{cr} is the root of the transcendental equation (2.6) in Ref. [5]. The saturation of the compressive force at the critical value (2.9a) has been verified numerically, see for example fig. 3.4 in Ref. [5], and the experimental results due to Ref. [6], see also fig. 3.1b in Ref. [3], indicate that the total tension $T_{TOTAL}(s,t)$ can be expressed in the form

$$\begin{aligned} T_{TOTAL}(s,t) = {} & \frac{1}{2}[1 + \mathrm{sign}(T(s) + \hat{T}_D(s,t) + P_{cr}(s))](T(s) \\ & + \hat{T}_D(s,t)) - \frac{1}{2}[1 - \mathrm{sign}(T(s) + \hat{T}_D(s,t) \\ & + P_{cr}(s))]P_{cr}(s), \end{aligned} \tag{2.9b}$$

where $T(s)$ is the static tension and $\hat{T}_D(s,t)$ is the dynamic tension (2.6b).

It follows then, from Eq. (2.9b), that the probability density function of the envelope of the maximum positive values of the dynamic tension can be approximated, even in this saturated situation, by Eqs. (2.6c), (2.7b), (2.8a) and (2.8b), as if the dynamical tension were effectively given by the quasi-harmonic expression (2.6b). This point will be numerically checked in the following section.

3. Numerical results

In all cases simulated the random sea was defined by a Pierson–Moskowitz spectrum with a cut-off frequency twice the peak frequency ω_P, see Ref. [2]. To characterize the sea state by a single parameter, the significant wave height H_S, the average wave steepness was assumed constant and equal to the value related to a fully developed sea, see Ref. [7], or

$$\delta_P = \frac{\omega_P^2 H_S}{g} = 0.24. \tag{3.1a}$$

The wave spectrum being then given by

$$S(\omega) = \frac{5}{16}\frac{H_S^2}{\omega_P}\frac{1}{\xi^5}\exp\left(-\frac{5}{4}\frac{1}{\xi^4}\right), \qquad 0 \le \xi = \frac{\omega}{\omega_P} \le 2. \tag{3.1b}$$

In the simulations an actual VLCC, with a turret placed at 0.2 L (or at 0.4 L) ahead the midship and anchored in a water depth $h = 1000$ m, was choosen as a floating system. The wave direction, measured in relation to the ship's axis, was $\beta = 180, 135, 90°$ and the significant wave height was taken in the interval $5\ \mathrm{m} \le H_S \le 14\ \mathrm{m}$; the cables, hanging from the turret center, have angles at the suspended end in the range $50° \le \theta_S \le 85°$. The transfer function (RAO) was determined by the program WAMIT and in all cases analyzed the tangent motion at the cables suspended end have a non-dimensional bandwidth in the range $0.10 \le \nu_U \le 0.16$, the smaller values being for $\beta = 90°$ and the larger ones for $\beta = 180°$. The properties of the cables, if a flexible riser or a steel riser or even an heterogeneous mooring line, are defined in Ref. [3], together with the ocean current profile. The cases selected to be discussed here are defined in Table 1; in all these cases $\beta = 90°$ since then the imposed motion is the largest one.

In case 1 the heterogeneous mooring line was not dynamically compressed and the dynamic tension can then be expressed in the form (2.6b). Fig. 1 shows, in the upper part, a window of the time series of the dynamic tension obtained directly from ORCAFLEX. This signal has been filtered then at the same cut-off frequency $2\omega_P$ of the wave spectrum, accordingly to the procedure suggested by Longuet-Higgins [2]; notice, also, that this filtering process has an experimental support since the presence of higher harmonics were not noticeable in the experiments done by Andrade [6]. The filtered signal is shown in the second row of Fig. 1 and the related envelope, obtained from the Hilbert transform (see Eqs. (2.3b) and (2.3c)), is shown in the third row; the last row in this figure shows the filtered signal superposed to the envelope.

Table 1
Cases simulated. H_S: significant wave height; β: incidence angle; h: water depth; (HL): heterogeneous mooring line; (FR): flexible riser; (SR): steel riser; θ_S: angle at the top (before the ocean current is turned on in cases 4 and 6). Turret at 0.2 L (in case 2 at 0.4 L)

Case	Environment			Cable			Tangent motion		
	H_S (m)	β (deg)	Curre.	Type	θ_S (deg)	h (m)	σ_U (m)	ω_U (rad/s)	ν_U
1	10	90	No	(HL)	58	1000	2.60	0.4838	0.10
2	10	90	No	(FR)	85	1000	3.45	0.4900	0.10
3	9	90	No	(SR)	60	1000	2.24	0.4913	0.10
4	9	90	Yes	(SR)	60	1000	2.3	0.4913	0.10
5	9	90	No	(SR)	73	1000	2.47	0.4915	0.10
6	9	90	Yes	(SR)	73	1000	2.52	0.4916	0.10

The probability density function was estimated from the obtained envelope record by observing the frequency of occurrence of tension's values at a sequence of discrete time intervals. To obtain some statistical stability it is desirable to average the numerical values, either using distinct set of simulations or else an extremely long simulation; since this procedure is very time consuming and several cases were analysed, the time record was assumed equal to 20 min in each simulation and some degree of uncertainty should be expected. Only in one case, just for this heterogeneous line, a second random simulation was computed and the numerical estimate of the probability density function was obtained from the average of the two simulations. The result is shown in Fig. 2, where the numerically estimated pdf, both at the TOP (suspended end) and TDP (touchdown point), is compared with Eq. (2.8b). The agreement is fair, in the sense that both the numerically estimated pdf and Eq. (2.8b) deviate from Rayleigh distribution in a similar way and that the two distributions are closer in the case where the average of the two simulations was taken.

In the right part of the same Fig. 1 a different plot is shown: there the cumulative probability function (cpf) is plotted against the dynamic tension normalized by its rms; in fact, what was plotted is the variable sqrt[$-2\ln(1-\text{cdf})$], that is exactly equal to the normalized tension for a Rayleigh distribution. In this plot the numerical values of sqrt[$-2\ln(1-\text{cdf})$] were computed by determining the frequency of occurrence of the *local maximum values* of the unfiltered Orcaflex time series (first row in Fig. 1)) and, once these discrete values are obtained, a Weibull distribution was fitted using a minimum square technique, see Refs. [8,9]. In the same figures the results obtained from Eq. (2.8b) are also shown and it is not difficult to explain the necessity of this plot here: in fact, as it will be seen, when the riser becomes dynamically compressed the approach based on the *envelope* ceases to be valid but the one based on the *local maximum* continue to be applicable. Furthermore, this plot is useful to check the behavior at the extreme values, where the probability density function is small.

The agreement between Eq. (2.8b) and the numerical results (and also with the Weibull distribution) in the plots of sqrt[$-2\ln(1-\text{cdf})$] is fair enough: both deviate from Rayleigh distribution in a similar way and show a relatively close agreement mainly for the extreme values of the normalized tensions. Besides eventual numerical inaccuracies, the result could be bettered by increasing the simulation time in order to obtain greater statistical stability.

In all remaining cases of Table 1 the cable becomes dynamically compressed both at the TOP and TDP (in case 2 only at the TDP) and this poses some questions in the procedure to estimate numerically the statistical properties. In fact, as the dynamical tension saturates at the critical value $-P_{cr}$ in the compressed zone, the signal ceases to be narrow banded and the approach used to estimate the envelope's probability density function looses its meaning: the envelope computed from the Hilbert Transform tries to cope with the well behaved narrow banded signal in the positive side and the saturated signal in the compressed part.

One must use then the other approach, based on the frequency of occurrence of the *local maximum* of the time signal, but even here the analysis is not as straight as before. Indeed, the normalized probability density function (2.8b) uses the normalized variable r, determined from Eq. (2.8a), with the rms computed from Eq. (2.6c), as if the dynamic tension were not saturated in compression. The point is that the actual rms should be computed from Eq. (2.9b) and the rms determined from ORCAFLEX should approach this value and not from Eq. (2.6c). Instead of computing the rms from Eq. (2.9b) an easier approach was followed here: the variable sqrt[$-2\ln(1-\text{cdf})$] was plotted, in the theoretical computation, as a function of r^* where

$$r^* = \frac{(\text{rms})_{(2.6c)}}{(\text{rms})_{\text{ORCA}}}\, r.$$

The theoretical dynamical tension has been normalized then by the rms obtained directly from ORCAFLEX, in such way that an eventual agreement between the numerical results and Eq. (2.8b) in the figures below means equal

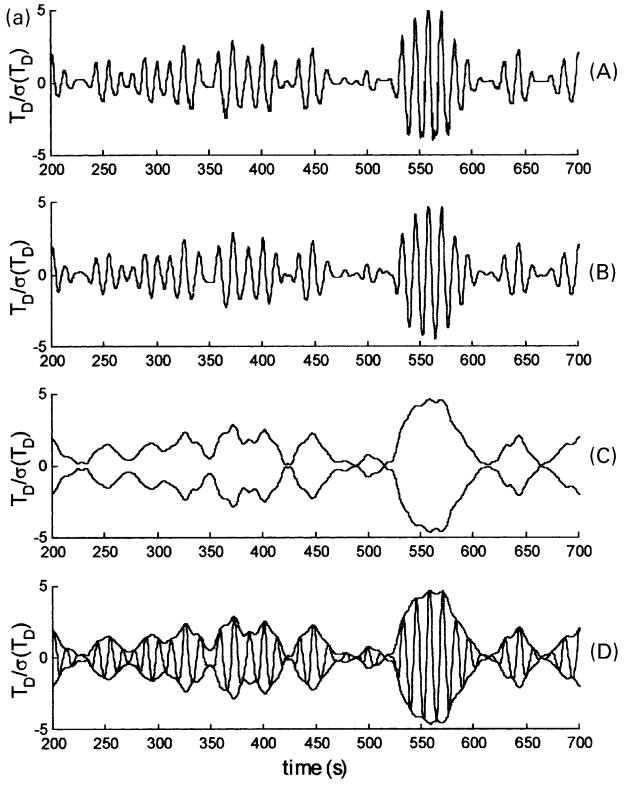

Fig. 1. Case 1: (a) (A) Orcaflex time series for the dyanmic tension (window); (B) filtered Orcaflex time series at $2\omega_P$; (C) envelope of (B) from Hilbert transform; (D) (B) + (C). (b) TOP. Left: envelope pdf: (—) (2.8b); (∗) Orcaflex (20 m); (○) Orcaflex (60 m); (- - -) Rayleigh. Right: (—) (2.8b); (◇) Orcaflex (20 m); (-·-·-) Weibull; (- - -) Rayleigh. (c) TDP. Left: envelope pdf: (—) (2.8b); (∗) Orcaflex (20 m); (○) Orcaflex (60 m); (- - -) Rayleigh. Right: (—) (2.8b); (◇) Orcaflex (20 m); (-·-·-) Weibull; (- - -) Rayleigh.

probability for the same level of the actual (dimensional) tension.

Fig. 2 shows, for the case 2, the plot of sqrt[$-2\ln(1-\text{cdf})$] as a function of the dynamic tension normalized by $(\text{rms})_{\text{ORCA}}$. The values have been obtained either from Eq. (2.8b) or by the frequency of occurrences of the local maximum in the simulation or else by the Weibull's fit of the numerical data; Figs. 3–6 show the same plot for the cases 3–6 defined in Table 1.

The agreement for case 2 (flexible riser) is good at the TDP and only fair at the TOP. Since the cable is dynamically compressed at the TDP, high frequency components generated there are propagated to the TOP, as discussed in Ref. [3], and may be the reason for the observed discrepancy. This possible explanation is reinforced by the following observation: the generation of the high frequency components are attenuated in a steel riser and, perhaps for this reason, the results from case 3 to case 6 show now a good agreement both at the TDP and at the TOP, in despite of the fact that the riser is dynamically compressed at both ends in all these cases. Notice that the agreement is good irrespective of the presence (or not) of an ocean current.

In general the agreement is fair enough, even more if the inaccuracies of the numerical solutions are accounted for and the fact that the time series were relatively short (20 m) is recalled. The probability density function here derived may be useful in the fatigue analysis of the cables and can give an immediate answer to an important question: to determine the probability for the envelope $T_{\text{D}}(s,t)$ to be larger than a reference value T_{R}. The inverse question has, however, a very simple answer as explained next.

In fact, let $U_{\text{R}}(\alpha)$ be the amplitude of the tangent displacement such that $\text{Prob}[U(t) > U_{\text{R}}(\alpha)] = \alpha$; given the *harmonic input* $\{\omega_U; U_{\text{R}}(\alpha)\}$ let then $T_{\text{R}}(s;\alpha)$ be the amplitude of the related tension at the section s. Since the basic input, the tangent motion, is *narrow banded* with central frequency ω_U and, for a given ω_U, the amplitude of the harmonic tension should *increase monotonically* with the amplitude of the imposed motion, then one must have, necessarily, that $\text{Prob}[T_{\text{D}}(s,t) > T_{\text{R}}(s;\alpha)] = \alpha$. This result does not depend on any mechanical model for the cable

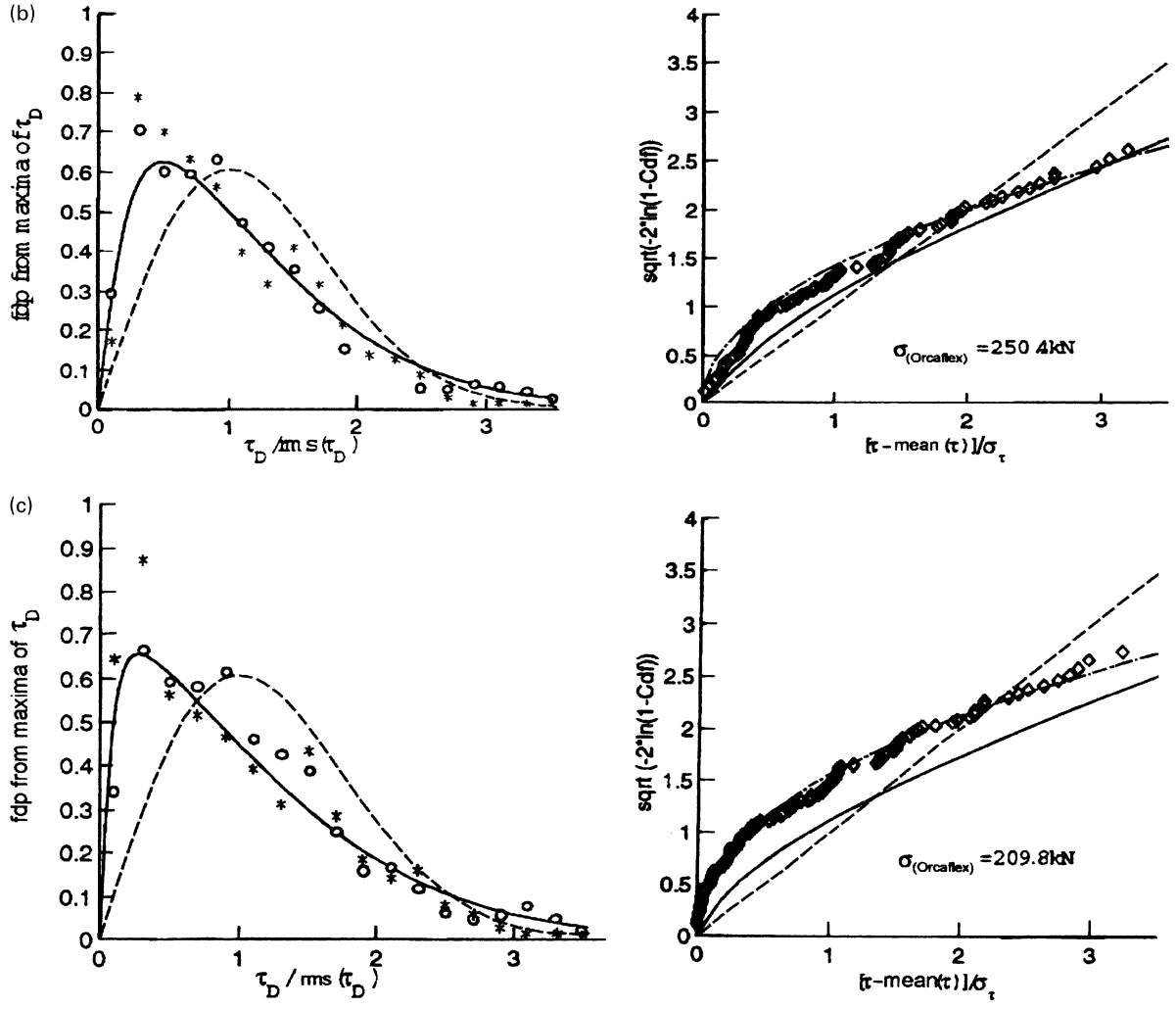

Fig. 1. (*continued*)

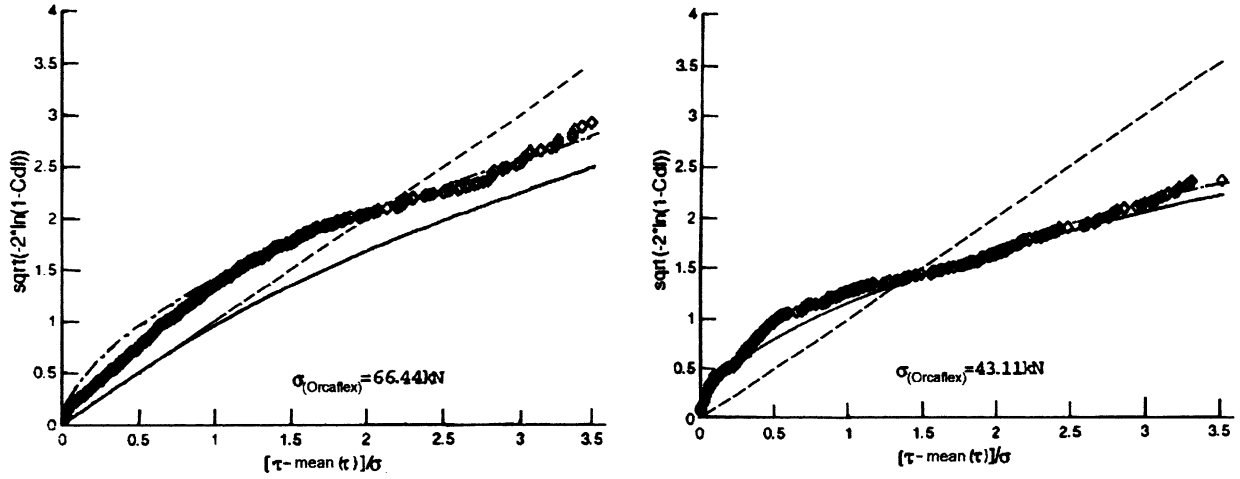

Fig. 2. Case 2. Left: TOP; Right: TDP. (—) (2.8b); (◇) Orcaflex (20 m); (-···-) Weibull; (- - -) Rayleigh.

dynamics and it is based only on two weak assumptions, namely: that the *imposed motion* at the suspended end is *narrow banded* and that the amplitude of the tension in an harmonic problem *increases monotonically* with the amplitude of the imposed motion. This is a strict justification for a popular way to estimate maximum tensions, within an acceptable probability α, using only the Rayleigh distribution for the tangent motion and the harmonic response of the cable.

4. Conclusions

An analytic approximation for the probability density function of the dynamic tension envelope was derived in this work, using the harmonic algebraic approximation derived in Ref. [3] and the assumption of a narrow banded input at the suspended end. In despite of possible numerical inaccuracies, mainly when the cable is dynamically compressed at the TDP, and eventual statistical fluctuations due to the short time records used, the agreement with numerical results is fair in general, becoming in fact fairly good for the steel risers, where the influence of the spurious high frequency oscillations in the numerical solutions is known to be weaker.

The obtained expression can be used even when the cable becomes dynamically compressed and the total tension saturates, in the compressed part, at the critical value (2.9a): as suggested by the experimental results due to Andrade [6], the maximum positive values of the dynamic tension are not substantially affected by the saturation phenomenon and the pdf of the maximum values can be well estimated by Eq. (2.8b).

The proposed expression may also be useful to address more involved statistical problems, related to the coupling analysis of the non-gaussian slow drift motion with the wave frequency dynamic tension, as addressed in a related context by Naess [10–12]; furthermore, it may be helpful to check the order statistics approach, proposed by Liu and Bergdahl [13], that can be a useful strategy in dealing with a non-narrow banded input.

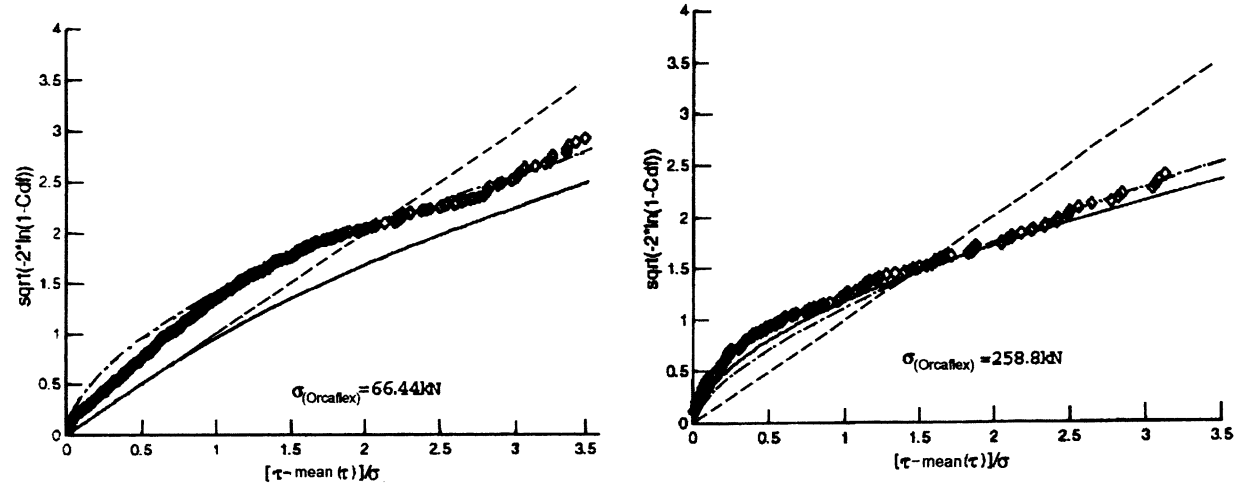

Fig. 3. Case 3. Left: TOP; Right: TDP. (—) (2.8b); (◇) Orcaflex (20 m); (-···-) Weibull; (- - -) Rayleigh.

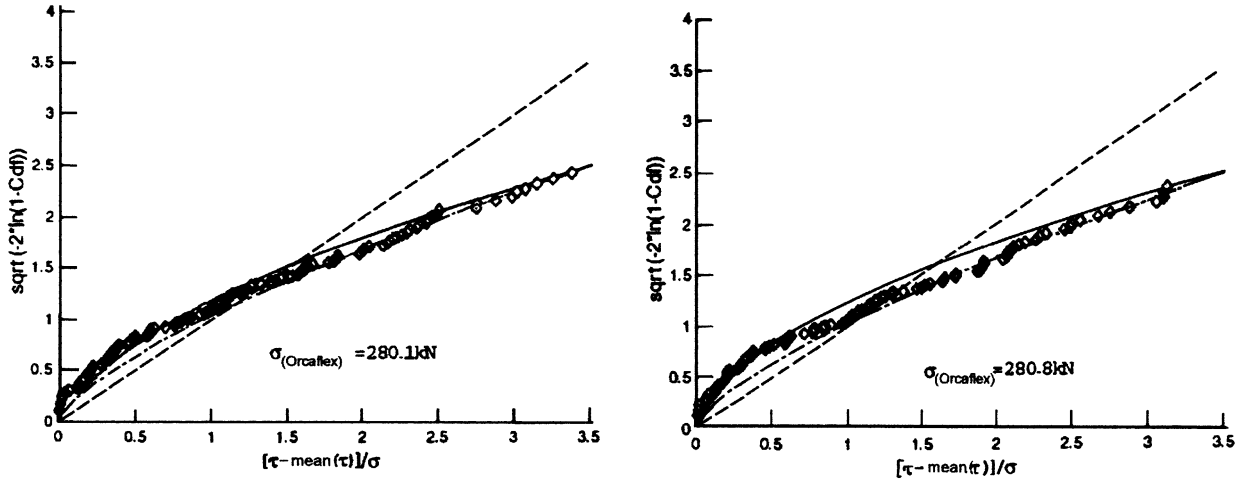

Fig. 4. Case 4. Left: TOP; Right: TDP. (—) (2.8b); (◇) Orcaflex (20 m); (-·-·-) Weibull; (- - -) Rayleigh.

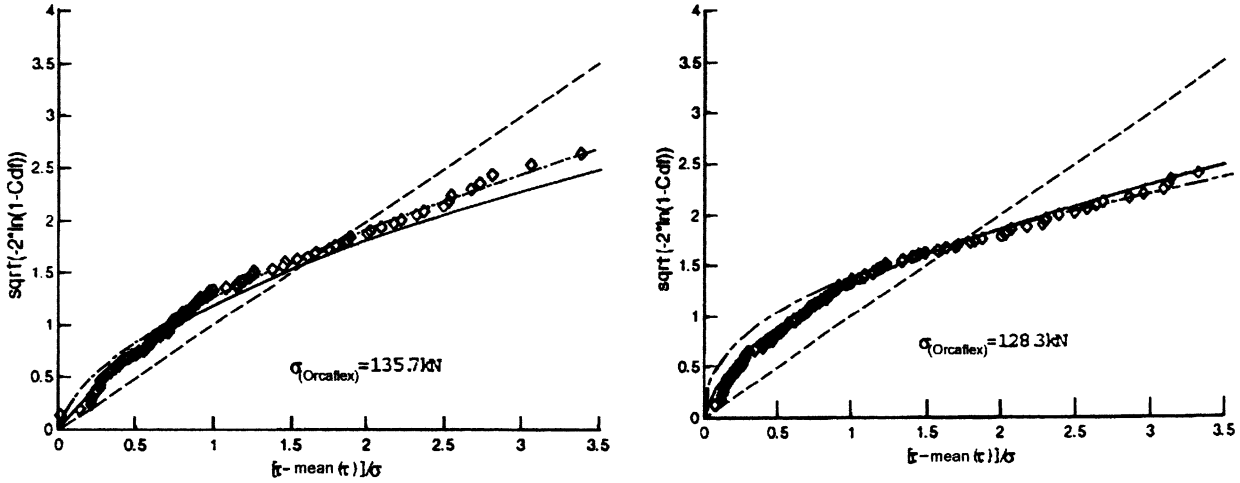

Fig. 5. Case 5. Left: TOP; Right: TDP. (—) (2.8b); (◇) Orcaflex (20 m); (-·-·-) Weibull; (- - -) Rayleigh.

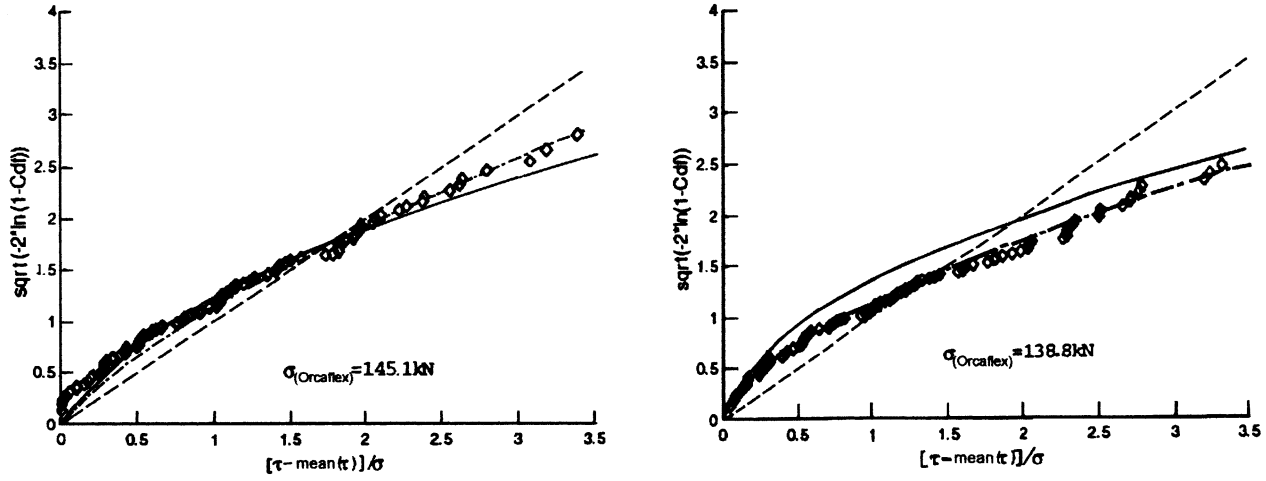

Fig. 6. Case 6. Left: TOP; Right: TDP. (—) (2.8b); (◇) Orcaflex (20 m); (-·-·-) Weibull; (- - -) Rayleigh.

References

[1] Longuet-Higgins MS. The statistical analysis of a random moving surface. Proc R Soc Lond A 1957;249:321–87.
[2] Longuet-Higgins MS. Statistical properties of wave groups in a random sea state. Philos Trans R Soc Lond A 1984;312:219–50.
[3] Aranha JAP, Pinto MO. Dynamic tension in risers and mooring lines: an algebraic approximation for harmonic excitation, 2001, submitted for publication.
[4] Triantafyllou MS, Bliek A, Shin H. Dynamic analysis as a tool for open-sea mooring system design. Presented at the Annual Meeting of the Society of Naval Architects and Marine Engineers, New York, 1985.
[5] Aranha JAP, Pinto MO, da Silva RMC. On the dynamic compression of risers: an analytic expression for the critical load, 2001, submitted for publication.
[6] Andrade BLR. Estudo experimental do comportamento dinâmico de linhas de amarração, Tese de Mestrado, Departamento de Engenharia Naval e Oceânica, EPUSP, 1993.
[7] Phillips OM. The dynamics of the upper ocean. Cambridge: Cambridge University Press, 1980.
[8] Siqueira MQ. Random fatigue analysis of a steel catenary riser in frequency and time domain. International Symposium on Offshore Eng., Brasil Offshore'97, Rio de Janeiro, Brazil, 1997.
[9] Zurita BIG. Estatística de Extremos de Séries Temporais Gaussianas e Não Gaussianas, M.Sc. thesis, Civil Engineering, COPPE/UFRJ, Rio de Janeiro, Brazil (in Portuguese), 1999.
[10] Naess A. Statistical analysis of second-order response of marine structures. J Ship Res 1985;20(4):270–84.
[11] Naess A. The statistical distribution of second-order slowly-varying forces and motions. Appl Ocean Res 1986;8(2):110–8.
[12] Naess A. Prediction of extremes of combined first-order and slow-drift motions of offshore structures. Appl Ocean Res 1989;11(2):100–10.
[13] Liu Y, Bergdahl L. Extreme mooring cable tension due to wave-frequency excitations. Appl Ocean Res 1998;20:237–49.
[14] Born M, Wolf E. Principles of optics. New York: Pergamon Press, 1975.